Chromium (VI) Separation from Aqueous Solution Using Anion Exchange Membrane

G. Pugazhenthi and Anil Kumar
Dept. of Chemical Engineering, Indian Institute of Technology, Kanpur, India 208016

DOI 10.1002/aic.10466
Published online May 16, 2005 in Wiley InterScience (www.interscience.wiley.com).

The preparation is reported of a chemically modified crosslinked poly(methyl methacrylate–ethylene glycol dimethacrylate) (PMMA–EGDM) copolymer anion exchange ultrafiltration membrane on a macroporous clay support. This is obtained by nitrating a PMMA–EGDM membrane using NO_x (a mixture of NO and NO_2), which is further reduced to an amine group using hydrazine hydrate to form an anion-exchange membrane (AEM). The membrane thus formed is characterized for its properties such as ion-exchange capacity, membrane swelling, contact angle measurements, and membrane morphologies. The results show that the membrane becomes highly hydrophilic on the introduction of a charge and the separation experiments on the chromium (VI) salt solution show that the permeate flux (keeping the same rejection level of 90%) is considerably increased (by 100-fold). The analysis of separation of Cr(VI) from its aqueous solution has been done by solving a two-dimensional (in cylindrical coordinates) space-charge model (SCM). A series solution of the nonlinear Poisson–Boltzmann equation has been generated, which leads to a considerable reduction in the computational time (from 15 h of batch time using the method reported earlier to 15 min for our method). The effective pore radius and wall potential of the unmodified and AEMs are evaluated by fitting the experimental data of the separation. The permeate flux calculated from this model matches well with the experimental values and a correlation is developed between the separation characteristic (rejection) and the wall charge developed by the chemical modification of the membrane. © 2005 American Institute of Chemical Engineers *AIChE J,* 51: 2001–2010, 2005

Keywords: ultrafiltration, space charge model, chromium (VI), AEM

Introduction

Composite membranes consist of two layers of different materials and are commonly used in many separation processes such as ultrafiltration, nanofiltration, and reverse osmosis.[1] Such membranes are formed by the deposition of a thin polymeric film on metal or ceramic macroporous supports. Some of the preparation techniques (to form a crack-free film on the support) are the dip coating method,[2] solution-deposition technique,[3] vapor deposition,[4] plasma-initiated polymerization,[5,6] photoinitiated polymerization,[7] radiation polymerization,[8] and interfacial polymerization.[9] Polymers used in the composite membranes include cellulose acetate,[10-12] styrene–acrylonitrile copolymer,[13] and polysulfone.[14] Recently, glassy materials have gained importance[15-17] with respect to which there are reports of using blends of poly(methyl methacrylate) (PMMA) with cellulose acetate,[18] bisphenol chloral polycarbonate,[19] poly(vinylidene fluoride) (PVDF),[20] and poly(dimethylsiloxane) (PDMS) grafted PMMA.[21,22]

Separation depends on the properties of the surface and is affected by such physicochemical properties as pore size, wettability, permeability, adhesion, or compatibility. To obtain a given set of properties, in recent years, chemical modifications of membranes have been carried out using crosslinking,[23] ra-

Correspondence concerning this article should be addressed to A. Kumar at anilk@iitk.ac.in.

diation grafting,[24] surface oxidation,[25] plasma-phase reaction,[26-29] and copolymerization. Gancarz et al. modified the ultrafiltration polysulfone membranes by plasma treatment using CO_2,[26] acrylic acid,[27] nitrogen,[28] and ammonia[29] and showed an increase in the pore size and wettability. In recent applications, some of the authors have chemically modified the polymeric membranes by chloromethylation and subsequently quaternized it.[30-35] Tongwen et al.[36] prepared a chemically crosslinked anion exchange membranes from linear poly(2,6-dimethyl-1,4-phenylene oxide) (PPO) and carried out the bromination reaction followed by amination.

The discharge of wastewater polluted with toxic metal into the environment is strictly controlled by legislation. The development and application of an effective treatment process is very important. Several methods have been reported in use for the control of metal toxicants. The most commonly applied physicochemical treatment methods are (1) precipitation as hydroxides, carbonates, or sulfides; (2) sorption (adsorption, ion exchange); (3) membrane processes; (4) electrolytic recovery; (5) evaporation; and (6) liquid–liquid extraction.[37-40]

In this work, we have prepared a charged crosslinked PMMA–ethylene glycol dimethacrylate (EGDM) clay composite membrane by nitrating (using the procedure of Neelakandan et al.[41]) and then aminating it using hydrazine hydrate.[42-48] Experiments were carried out for separation of Cr(VI) from its aqueous solution and to examine the effect of modification on the membrane properties including water uptake, anion-exchange capacity, contact angle, and membrane morphologies. We have modeled the membrane performance on separation of Cr(VI) using a two-dimensional space-charge model and determined the effective pore radius and the wall charge of these membranes.

Space-Charge Model (SCM)

The charges on the membrane are known to substantially affect their separation properties and fouling tendency because of the electrical interaction between membrane wall charge and ionic solutes.[49] For neutral solutes, the electrical interaction occurs as a result of nonzero average of the induced instantaneous dipole moment and polar–polar interaction. The fixed-charge model, proposed by Teorell[50] and Mayer and Sievers[51] (TMS model), has been used to describe the rejection of charged ultrafiltration membranes.[52] It assumes a fixed wall charge density and a uniform radial distribution of potential and ion concentration and is independent of the pore structure. A more realistic two-dimensional (in cylindrical coordinates) model, known as the space-charge model (SCM), was originally developed by Osterle and co-workers.[53,54] According to this, the membrane is visualized as a bundle of cylindrical capillaries in which variation of the potential and concentrations in the radial direction occurs. The basic equations of the SCM are the nonlinear Poisson–Boltzmann equation for the radial distribution of potential and ion concentration (Eq. 3 of Shukla and Kumar[55]), the Nernst–Planck equation for ion transport (Eq. 1 of Shukla and Kumar[55]), and the Navier–Stokes equation for volumetric flow (Eq. 2 of Shukla and Kumar[55]).[56] The model involves coupled nonlinear differential equations and is highly computationally intensive.[57-62]

The system of governing equations represents a set of coupled nonlinear differential equation that is solved by making suitable assumptions and writing in terms of dimensionless quantities. The nondimensional Poisson–Boltzmann equation for the symmetric electrolytes (Eq. 4 of Shukla and Kumar[55]) can be written as[55,56]

$$\frac{1}{\eta}\frac{\partial}{\partial \eta}\left(\eta \frac{\partial \bar{\psi}}{\partial \eta}\right) = \frac{1}{\lambda^2}\sinh(\bar{\psi}) \tag{1}$$

where

$$\bar{\psi} = \frac{F\psi}{\Re T} \qquad \eta = \frac{r}{a} \qquad \lambda = \frac{\kappa}{a} \qquad \kappa = \left[\frac{\varepsilon \Re T}{2F^2 c(x)}\right]$$

The boundary conditions of the equation are

$$\left.\frac{\partial \bar{\psi}}{\partial \eta}\right|_{\eta=0} = 0 \tag{2a}$$

$$\bar{\psi}|_{\eta=1} = \bar{\psi}_w \tag{2b}$$

or

$$\left.\frac{\partial \bar{\psi}}{\partial \eta}\right|_{\eta=1} = \bar{q} = \frac{Fqa}{\varepsilon RT} \tag{2c}$$

where ψ is that part of the electrostatic potential that depends both on x and r variables. The above equations were solved simultaneously to determine the wall charge/wall potential of the pores, permeate flux [related to the Peclet number (Pe)] and rejection (related to the solute flux) of the membrane. The detailed series solution of the nonlinear Poisson–Boltzmann equation (Eq. 1) was presented in our earlier work[55] and is given by

$$\sum_{i=0}^{\infty}(i+2)^2 a_{i+2}\eta^i = \frac{1}{\lambda^2}\sum_{\alpha=0}^{\infty}\frac{\sum_{i=0}^{\infty} a_{i,\alpha}\eta^i}{(2\alpha+1)!} = \frac{1}{\lambda^2}\sum_{\alpha=0}^{\infty}\sum_{i=0}^{\infty}\left(\sum \frac{C a_j^r a_k^s a_l^t \cdots}{r!s!t!\cdots}\right)\eta^i = \frac{1}{\lambda^2}\sum_{i=0}^{\infty}\sum_{\alpha=0}^{\infty}\left(\sum \frac{C a_j^r a_k^s a_l^t \cdots}{r!s!t!\cdots}\right)\eta^i \tag{3}$$

where $r + s + t + \cdots = 2\alpha + 1$ and $j + k + l + \cdots = i$.

The coefficient of η^i on left- and the right-hand sides of the above equation should be equal and, on comparing them, the relationship among the a_i parameters can be obtained (reported in Shukla and Kumar[55]). The algorithm for solving the space-charge model equation was introduced in our earlier work.[55]

Table 1. Reflection Coefficient, Solute Permeability, Hydraulic Resistance, Effective Pore Radius, and Wall Potential of the Membranes

Type of Membranes*	Reflection Coefficient, σ	Solute Permeability, P_m (L h^{-1} m^{-2})	Hydraulic Resistance, R_m (kPa h^{-1} m^{-2} L^{-1})	Effective Pore Radius from SCM (nm)	Wall Potential from SCM (ψ_w)
Unmodified membrane	0.97	0.13	1316	1.0	2.1
3-AEM	0.90	0.21	47	3.5	2.4
6-AEM	0.87	1.04	29	6.0	4.37
9-AEM	0.82	1.17	23	6.5	4.15

*AEM (anion-exchange membrane): nitrated for different durations (3, 6, and 9 h) and aminated for 8 h at 50°C.

Experimental

Preparation of anion exchange PMMA–EGDM clay composite membrane

Ceramic supports of the circular disc are prepared by mixing the following clay mixtures: kaolin [$Al_2(Si_2O_5)(OH)_4$, 13.28 g], ball clay ($3SiO_2Al_2O_3$, 16.15 g), feldspar [(Na,Ca)-($AlSi_3O_8$), 5.15 g], quartz (SiO_2, 24.44 g), pyrophyllite [$Al_2(Si_2O_5)_2(OH)_2$, 13.54 g], and calcium carbonate ($CaCO_3$, 27.44 g) with 60 g distilled water. The supports are first dried at ambient condition for 24 h, at 100°C for 24 h, at 250°C for another 24 h, and finally calcined at 900°C for 8–10 h.[41]

A mixture of methyl methacrylate (MMA; 0.0607 gmol) and EGDM (3.067×10^{-3} gmol) is copolymerized using dual initiators consisting of benzoyl peroxide (BPO; 3.388×10^{-4} gmol) and azobisisobutyronitrile (AIBN; 2.62×10^{-4} gmol) with an accelerator dimethyl aniline (DMA; 2.07×10^{-4} gmol) at room temperature. The above prepared copolymer solution is used to cast the polymer layer onto the clay support and was crosslinked at 60°C for 3 h to obtain a composite membrane [called an unmodified membrane (UM)]. It is then nitrated using NO_x (a mixture of NO and NO_2) at 100°C for different durations (3, 6, 9, and 12 h)[41] [called a nitrated membrane (NM)]. To prepare anion-exchange membranes, we introduced amine groups on the nitrated membrane by reducing the NO_2 group (3, 6, 9, and 12 h nitrated membrane[41]) using hydrazine hydrate at 50°C for 8 h.[41-48] These membranes were then treated with 0.1 N hydrochloric acid to obtain an anion-exchange membrane [AEM; hereafter, these are designated as 3-AEM, 6-AEM, 9-AEM, and 12-AEM (see Table 1)].

Characterization of membranes

To confirm the chemical modification, the FTIR spectra of the unmodified and aminated polymer samples were recorded in film form using a Perkin–Elmer system 1600 spectrometer (Perkin–Elmer Cetus Instruments, Norwalk, CT). Bond energies of the unmodified, nitrated, and aminated PMMA–EGDM polymer films were determined through electron spectroscopy for chemical analysis (ESCA) using a VG MK.II instrument (VG Scientific, East Grinstead, UK). Thermal properties of the polymer layer were investigated by thermal gravimetric analysis (TGA) and by differential scanning calorimetry (DSC). The TGA studies were carried out using a Perkin–Elmer TGA-6 instrument. Before analysis, the polymer samples were dried under vacuum at 60°C for 24 h and thermograms were obtained in the temperature range of 50–700°C at a constant heating rate of 20°C/min under nitrogen atmosphere.

To determine the water content, the polymer film was immersed in distilled water for 3 days and the wet film was weighed after wiping the surface with filter paper. This weighed wet polymer film was dried at a fixed temperature (75°C) for 6 h, after which the weight was determined. The mass of water lost by this procedure is termed *unbound moisture*. The remaining water present in the polymer film, which was found to be extremely difficult to remove, could nonetheless be removed after keeping the polymer sample in a vacuum dessicator for 6 months. This water (removed by keeping the sample in the dessicator) is called *bound water*. Earlier studies on PMMA–EGDM resin (1 mm size) have shown that it can be removed from a vacuum dessicator after about 6 months of storage.[47]

The anion-exchange capacity (AEC) of the membrane was determined by use of an ASTMD procedure[63] for the resin that requires regeneration of resin, which is done using mixed acid [18.1 mL of H_2SO_4 (sp gr. 1.84) with 27.5 mL of HCl (sp gr. 1.19)] of 1% concentration.[47] The aminated polymer film is kept in the mixed acid for 24 h after this, upon which it is washed with distilled water until the filtrate becomes neutral. The regenerated polymer film is then kept in 0.1 N $NaNO_3$ solution for 24 h, after which the solution is separated from the polymer film. The $AgNO_3$ (1.7 g) is added to this solution along with 2–3 drops of concentrated HNO_3 to bring the pH of the solution to 2.0. The entire content is again kept for 24 h, during which the chloride ions precipitate as AgCl, filtered, and weighed, and the AEC is calculated.

The physical parameter often used as an indication of susceptibility to fouling is the hydrophilicity/hydrophobicity of the membrane surface. The dynamic contact angle (θ) between water and the membrane surface was determined using a goniometer (Model 100-00-230, Ramé–Hart, Mountain Lakes, NJ). Measurements were carried out on both unmodified and anion-exchange PMMA composite membranes. To minimize the experimental error, the contact angle was measured 20 times for each membrane at different places and then averaged. The work of adhesion is given by[64]

$$w_A = \gamma_w(1 + \cos\theta) \tag{4}$$

where γ_w is the water surface tension (7.28×10^{-2} N/m). Values of w_A for different membranes indicate their hydrophilicity. The molecular weight cutoff (MWCO) of the modified membrane was carried out using a 1 wt % solution of different molecular weight poly(ethylene glycol) (PEG).[41]

Ultrafiltration experiment

The detailed batch cell experimental setup has been described in our earlier work.[41] The membrane area was 0.0036 m^2 and the temperature was kept at 25°C for all the experiments. All the membranes were compacted using water at 689 kPa before starting the experiments. After compaction, we measured the pure water flux (PWF) at different pressures and carried out the separation experiment with chromium (VI) salt solution (chromic acid). The observed and intrinsic rejection factor was determined using the irreversible thermodynamic approach (Spiegler–Kedem model) and the procedure described in our earlier paper.[41] Feed and permeate concentration was measured by a conductivity cell. For each run, the cell is filled with 250 mL of chromium (VI) salt solution (1000 ppm) and permeate flux is measured after 50 mL of permeate passed through the membrane. Permeate flux was calculated by measuring the time interval corresponding to 25 mL permeate volume.

Results and Discussion

Characterization of membranes

To confirm the presence of the NH_2 functional group on the modified membrane, we carried out FTIR analysis of the aminated PMMA–EGDM polymer film. The FTIR spectrum shows a broad band between 3600 and 3200 cm^{-1}, which may be attributed to stretching vibration of N–H bonds in amines, an additional N–H bend (scissoring) at 1557 cm^{-1}, and C–N stretching at 1193 cm^{-1}, which confirms the presence of NH_2 groups on the polymer matrix. To carry out the elemental analysis of aminated PMMA–EGDM membranes, we determined the binding energy of different elements present in PMMA–EGDM film samples. We examined the unmodified, nitrated, and aminated PMMA–EGDM samples for survey scan in the range of 0–500 and 500–1000 eV. We scanned carbon in the range of 265–315 eV and the C 1s peaks for the unmodified, nitrated, and aminated samples are observed at 284, 285, and 284.2 eV, respectively. The shifting in the peak portion of C 1s binding energy confirms the formation of C–N bonds. Figure 1 shows the individual scans of nitrogen in the range of 385–435 eV for nitrated and aminated PMMA–EGDM samples. A characteristic peak for N 1s appears at 401.2 eV for nitrated membrane, which is in the nitrogen range of 395–410 eV. This peak becomes broader in the aminated sample and appears at 404.5 eV, which confirms the formation of C–NO_2 and C–NH_2 bonds.

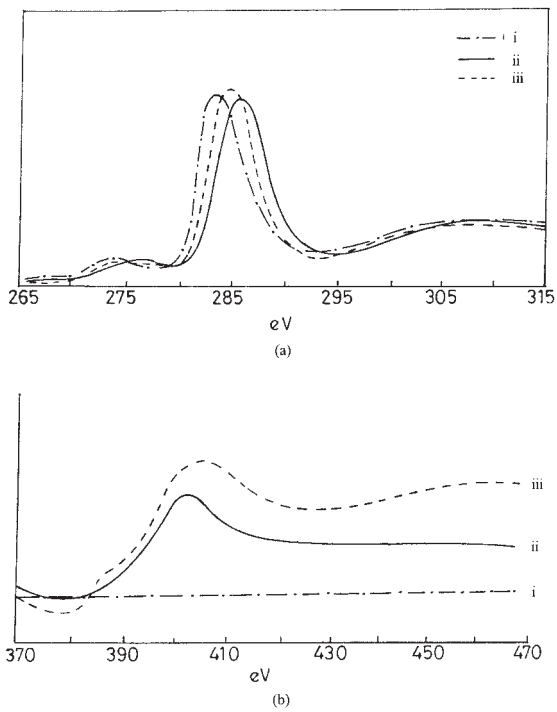

Figure 1. ESCA analysis of (i) unmodified, (ii) nitrated (3 h), and (iii) aminated (3 h) polymer film.

(a) 1s bond energy; (b) N 1s bond energy.

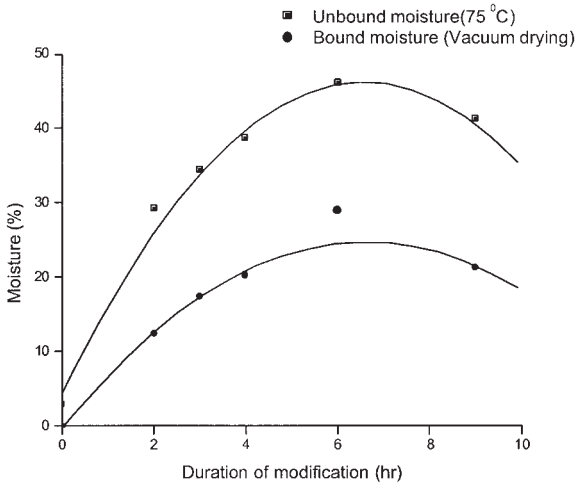

Figure 2. Variation of equilibrium moisture of AEM membranes with duration of modification.

Thermal Properties. We carried out the TGA analysis to show that there was no thermal degradation or decomposition of polymer at the modification reaction temperature. TGA analyses of all the polymer films show similar thermal properties up to a temperature of about 240°C and the weight lost is almost constant at temperatures $>$ 460°C. The DSC thermograms show that the unmodified, nitrated, and aminated polymer films have glass-transition temperatures (T_g) of about 133, 123.5, and 130.9°C, respectively.

Equilibrium Water Content. The swelling behavior of the membranes was investigated in terms of water content. The relation between the membrane water content and the duration of modification of membranes is shown in Figure 2. The unmodified membrane loses the absorbed water completely after being oven dried at 75°C. The water content was found to increase gradually with increasing duration of the modification reaction, which could be attributable to the presence of the polar amine group after amination. The results obtained here can be attributed to the increase in the hydrophilicity imparted to the membranes by the incorporation of amine groups with the increase in the duration of modification.

Anion-Exchange Capacity (AEC). Figure 3 shows the relationship between the AEC (meq/g of dry sample) and the duration of modification. It can be seen that the increase in the modification reaction time leads to a gradual increase in the

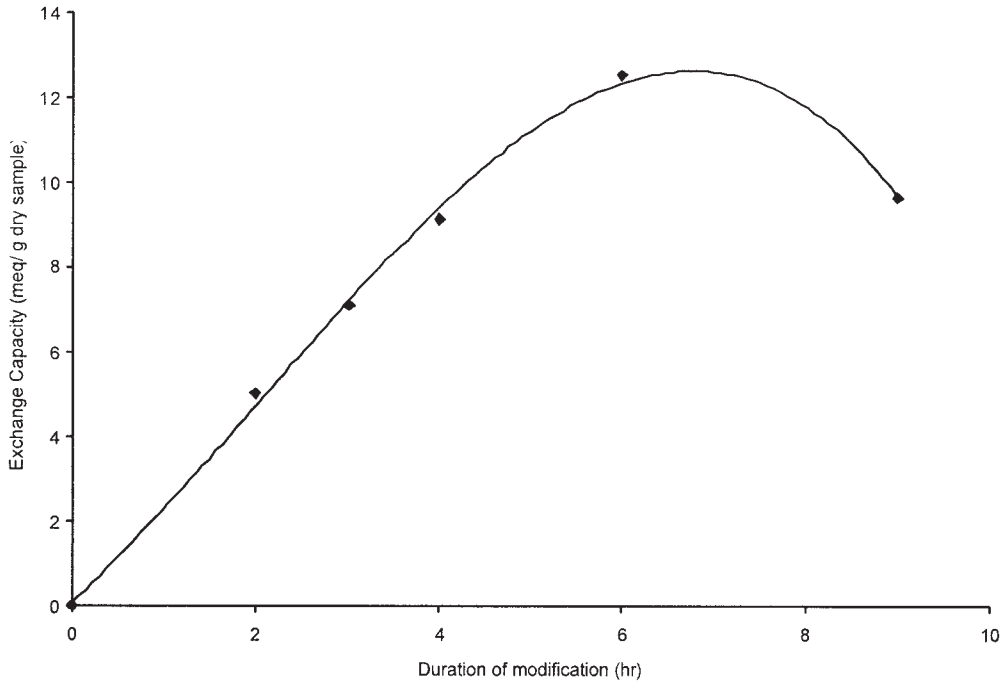

Figure 3. Relation between the anion-exchange capacity of the AEM membranes with duration of modification.

ion-exchange capacity. We find in Figure 3 that on increasing the reaction time, the amount of nitrate group on the polymer matrix increases and thus the exchange capacity also increases. After 6 h of modification reaction, there is a slight decrease in the ion-exchange capacity, which may be explained by the degradation of polymer during long modification time. We observe a maximum exchange capacity of 12.52 meq/g of dry sample after 6 h of modification. In our earlier studies on the modification of PMMA–EGDM resins, we showed that, if an amine group is present on all repeat units, the theoretical exchange capacity would be 6.64 meq/g of dry sample. The observed exchange capacity of the membrane is about thrice this value, which implies that the membrane thus prepared is highly nitrated (as a result of which it is highly charged). This higher capacity can be explained only by multiple nitration of a given repeat unit.[47] The other modification techniques reported in the literature[34-36] for the preparation of anion-exchange membranes have an exchange capacity of 0.5–3.7 meq/dry g of membrane, which is found to be considerably lower than that reported in this work.

Contact Angle. Contact angle studies were conducted to assess changes in the hydrophilicity arising from modification of the membranes. Figure 4 shows the dynamic contact angle values and the work of adhesion (w_A) of the unmodified (UM) and AEM membranes that were calculated from Eq. 4. We find that for the UM membrane it is 58.4°, which is consistent with the literature value of 57°.[65] The decline in the contact angle implies that there is an increase in the adhesion, attributed to an increase in the hydrophilicity stemming from the increase in the duration of modification.

Determination of Pore Size. The pore size of the membranes was estimated through the experimental determination of rejection of 1 wt % of a PEG solution in water.[41] Figure 5 shows the MWCO values of the UM, 3-AEM, and 6-AEM membranes: 8.5 kDa (mean pore size ~ 2.0 nm), 19.5 kDa (mean pore size ~ 4.5 nm), and 50 kDa (mean pore size ~ 9.5 nm), respectively. It is evident that the pore size of the membrane increases with the duration of modification.

Membrane performance

After compaction, the membranes were analyzed for pure water flux (PWF) at different applied pressures. Figure 6a shows the PWF as a function of applied pressure for the unmodified (UM) and anion-exchange membranes (AEM). It is evident from the figure that an increase in the applied pressure increases the PWF at a linear rate and obeys Darcy's law for all

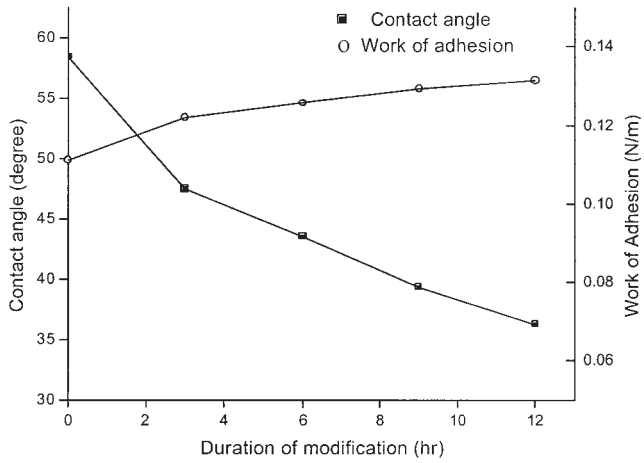

Figure 4. Variation of contact angle and work of adhesion of the AEM membranes with duration of modification.

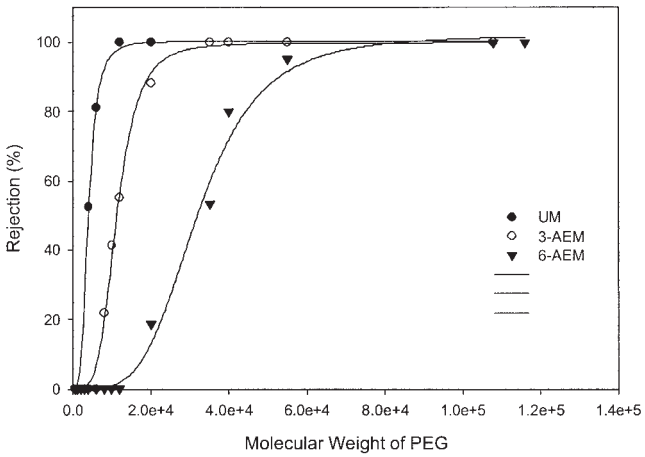

Figure 5. Molecular weight cutoff of the unmodified and anion-exchange membranes.

the membranes. It is found that the PWF of AEM is greater (by 75-fold) than that of the UM membrane, which is attributed to an increase in the pore size on modification. As a result, the transport resistance of AEM decreases, resulting in higher flux and lower membrane resistance (R_m) (Table 1). The hydraulic resistance (R_m) of the membranes was obtained by linear regression of pure water flux (J_v) vs. applied pressure (ΔP) and is given in Table 1. To show that the AEM membranes had greater advantage over the nitrated membrane (NM) reported in our earlier study,[41] we calculated the percentage increase in the flux, which is defined as

$$\text{Increase in water flux (\%)} = \left\{\frac{\text{AEM flux} - \text{NM flux}}{\text{NM flux}}\right\} \times 100 \tag{5}$$

where the NM flux has been taken from our earlier publication.[41] Figure 6b shows the percentage increase in the PWF of AEM membranes as a function of applied pressure; the PWF is found to increase dramatically compared to the NM membranes. We have shown that by amination, there is a nearly 15% increase in pore size and the hydrophilicity increases considerably. Figure 7a shows the chromium (VI) salt solution permeate flux as a function of the applied pressure for the UM and AEM membranes. It can be seen from the figure that the permeate flux is significantly affected by modification reaction. For 9-AEM, the permeate flux improved dramatically [100-fold higher than the UM and 40% higher than the nitrated membrane (NM),[41] tested for the same application], which means that the fouling of the membrane can be reduced by the modification reaction through formation of hydrophilic surface. Figure 7b shows that the percentage increases in chromium (VI) salt solution permeate flux of AEM membranes as a function of the applied pressure. The permeate flux was found to be lower than that of the pure water flux with increasing applied pressure, which implies that the presence of chromate ions generates additional resistance to the flow as a result of the electroviscous effect, defined as the increase in the apparent viscosity over the bulk value. The presence of an electrical double layer inside the pores exerts a profound influence on the behavior of the fluid flowing through the membrane pores.[70] The ions moving in the electric field will drag solvent molecules with them, thus changing the flow field of the liquid, resulting in an increased apparent viscosity.

Figure 8 shows that the chromium (VI) salt rejections as a function of applied pressure (ΔP) for all membranes. Intrinsic rejection was calculated using permeate flux and chromate concentration in the permeate by the procedure described in our earlier study[41] (Spiegler–Kedem model). It was found that the chromate concentration at the membrane surface was up to twofold higher than the concentration in the bulk. The observed rejection decreases for all the membranes with increasing applied pressure and the trend is the same as that reported in the literature.[37] It can be seen that the intrinsic rejection increases with increasing applied pressure, which is typically found in the separation of electrolytes through charged membranes. Table 1 gives the reflection coefficient σ and the solute permeability P_m, which is calculated from experimental data of the rejection; R and the permeate flux J_v were calculated by best-fit

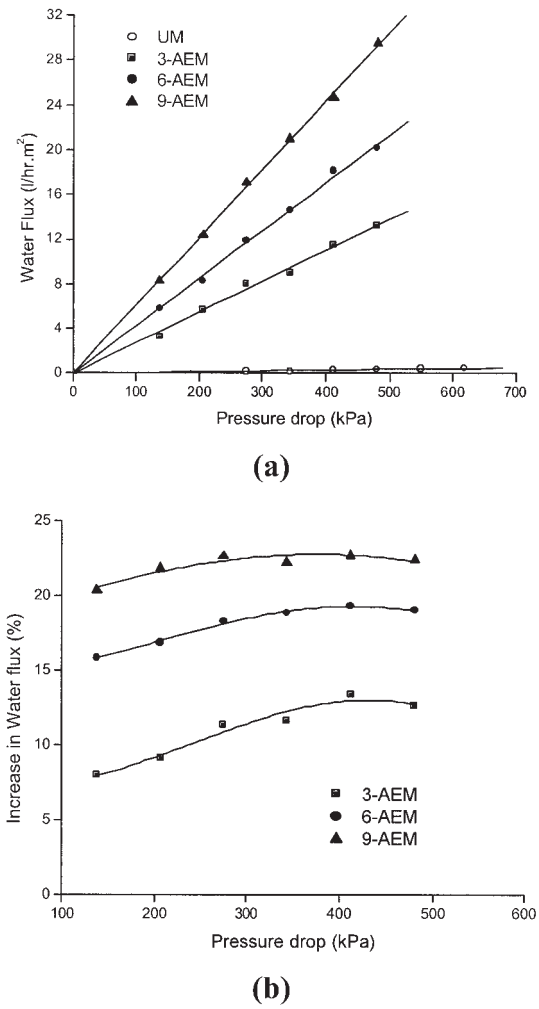

Figure 6. (a) Pure water flux as a function of pressure drop for the unmodified and modified membranes. (b) Percentage increase in the pure water flux (defined in Eq. 5) of AEM membranes as a function of pressure drop.

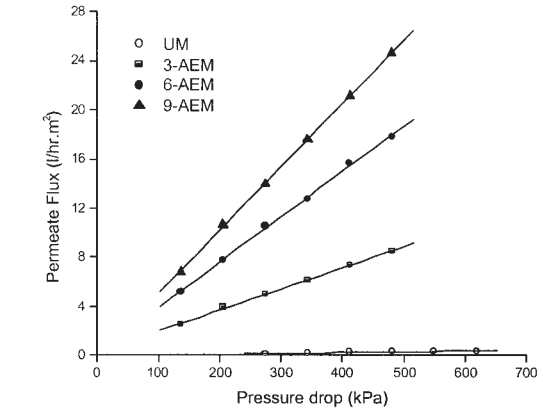

(a)

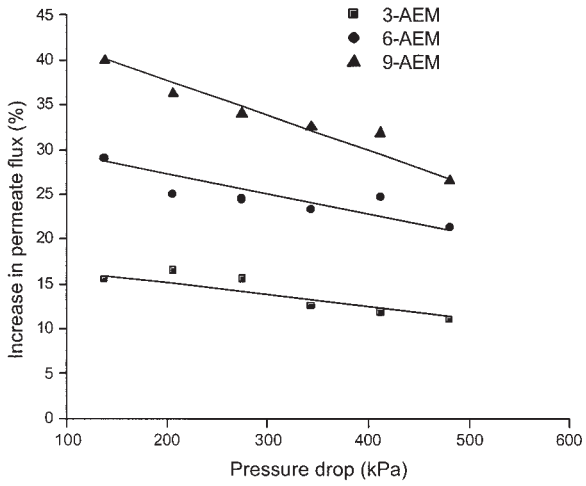

(b)

Figure 7. (a) Permeate flux of Cr(VI) as a function of pressure drop for the unmodified and anion-exchange membranes. (b) Permeate flux of Cr(VI) as a function of pressure drop for the AEM membranes. (Increase in permeate flux in percent is defined in Eq. 5.)

method. The value of σ for AEM membranes was found to be lower than the UM because of the increasing pore size as well as hydrophilicity.

Pollution control guidelines restrict the concentration of chromium in the effluent streams to extremely low values (<5 ppm), which can be achieved only by using expensive techniques of separation such as reverse osmosis and ion exchange. The utility of our modified membranes lies in lowering the load on the expensive reverse osmosis or ion-exchange unit. To compare membranes, a new parameter S_p (called the separation performance) is defined that combines both intrinsic rejection coefficient (R) and the permeate flux and is given by $S_p = J_v(C_m - C_p)$, where C_p and C_m are solute concentrations in the permeate and on the membrane surface, respectively. The S_p represents the total amount of solute separated by a given membrane per unit time. Figure 9 shows the S_p values as a function of applied pressure. The S_p values are higher (12-fold) for the modified membranes (AEM) compared to that of the

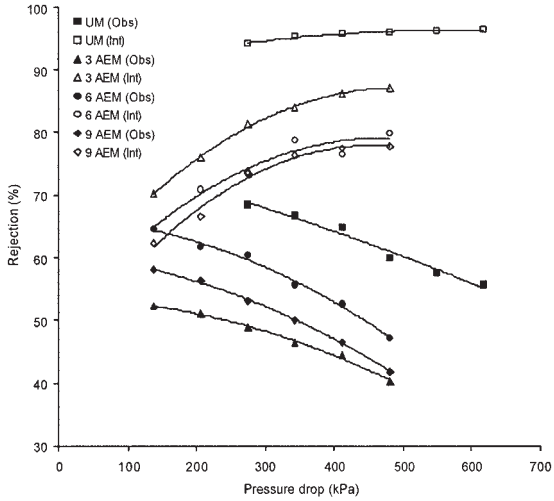

Figure 8. Observed (filled symbols) and the intrinsic rejection (open symbols) of Cr(VI) (calculated from Spiegler–Kedem model) as a function of pressure drop for the unmodified and anion-exchange membranes.

unmodified membrane (UM). This is because, even though the rejection coefficients of the modified membranes are lower, its fluxes are higher compared to those of the UM. This clearly indicates the improvement and importance of the modified membranes over the unmodified membrane.

In Sasidhar and Ruckenstein,[66] a theoretical space-charge model has been described and through detailed computations, the effect of pressure drop on the solute flux has been determined. The overall flow is governed by a combination of gradients of osmotic, applied pressure, and electrochemical potential and for $\Delta P = 0$, solvent flows from a region of low solute concentration to that of high concentration resulting from osmosis, whereas the solute permeates through the pore in the opposite direction. On increasing ΔP, the osmotic flow is reduced and there is a critical pressure for which the net volumetric flow reduces to zero. Upon further increasing the

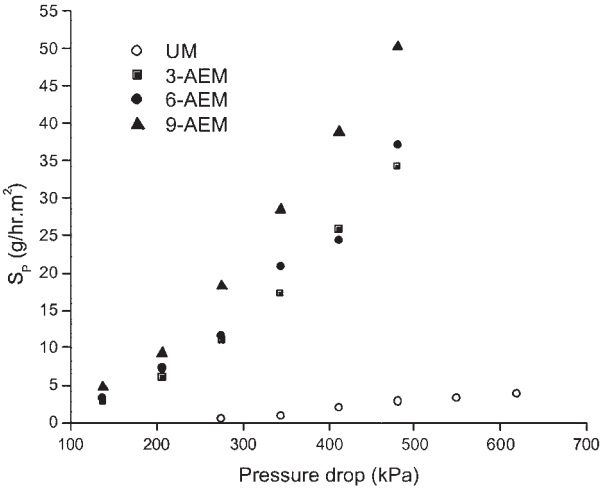

Figure 9. Separation performance (S_p) values as a function of applied pressure.

ΔP, the volumetric flow of the solvent and the solute flux takes place in the direction of decreasing concentration and is always less than the Poiseuille flow corresponding to the same ΔP. On further increasing ΔP, there is another critical value for which there is a decline in the solute flux resulting from the effect of electrical field on the velocity distribution of the fluid.

The observed rejections of all the membranes, as shown in Figure 8, are found to be significantly lower than the intrinsic rejections, consistent with the flow model presented earlier. This indicates that the concentration polarization effects are significant and lead to considerable loss of efficiency and, moreover, clearly shows that R_{obs} is strongly dependent on the operating conditions, whereas R_{int} accurately represents the intrinsic property of the membrane. The solute rejection by AEM depends on the charge of the ions, charge density on the pore walls of the membrane, pore size, and feed solute concentration. These membranes reject ionic solutes because of the phenomenon of Donnan ion exclusion. For a membrane containing fixed positive groups, the effect of Donnan potential is to repel cations or co-ions (ions with the same charge as that of the membrane) from the membrane and, because of the electroneutrality requirement, the solute is rejected.[67,68] For 9-AEM, the rejection is found to be less compared to that of the 6-AEM, which is likely to be the result of an increase in the pore size and slight decrease in the ion-exchange capacity (shown in Figure 3).

Modeling of membrane performance

The simulation is done on a Pentium IV PC using the MATLAB® 6.5 software (The MathWorks, Natick, MA). The tolerance value for the numerical calculation of the solution of the Poisson–Boltzmann equation is kept at 10^{-6}. The model requires the membrane properties (pore radius, membrane area, porosity, and pore length) and electrical (wall potential/charge) parameters. Pore size of the membrane has been determined by MWCO experiment (2.0, 4.5, 9.5, and 12.0 nm are for UM, 3-AEM, 6-AEM, and 9-AEM, respectively). Pore length of the membrane is taken as the thickness of the polymer layer and is found to be 40 μm.[41] To determine membrane porosity, the polymer layer was equilibrated in water; the volume occupied by water and the volume of membrane in the wet state were determined. The membrane porosity was defined as[71]

$$\text{Porosity } (\%) = \left[\frac{W_1 - W_2}{d_{water}}\right] \times \frac{100}{V} \tag{6}$$

where W_1 and W_2 represent the weights of the polymer films in the wet and dry states, respectively; d_{water} is the density of pure water at 20°C; and V is the volume of the polymer film in the wet state. Porosities of UM, 3-AEM, 6-AEM, and 9-AEM membranes were found to be 0.1, 0.15, 0.20, and 0.23, respectively. In our earlier publications,[55,56] we compared the accuracy of the series solution of the Poisson–Boltzmann equation with the numerical solution explained in detail. The space-charge model has been used to analyze the experimental data on the separation of Cr(VI) and evaluated the wall potentials and effective pore radius of the membranes. To show that the series solution dramatically reduces the computational load compared to that of the numerical integration, the Poisson–Boltzmann equation has been solved by two methods. The CPU time required is calculated as a function of wall charge and λ. For a typical simulation with the same initial values of pore size and wall potential, the time taken for series solution method is about 15 min compared to 15 h taken for the code (used in MATLAB® 6.5) that used numerical integration to determine a solution of the Poisson–Boltzmann equation.

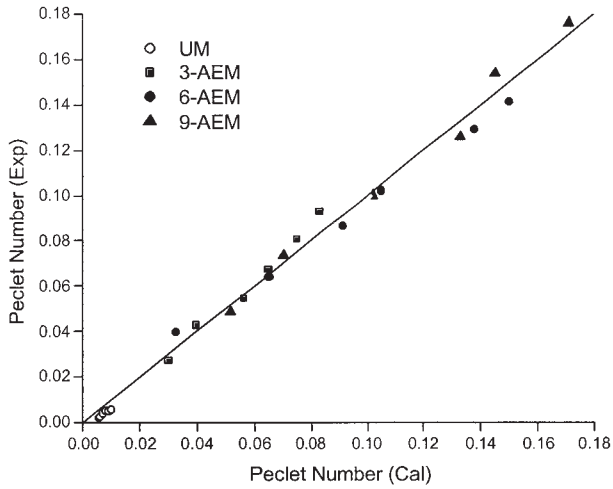

Figure 10. Comparison of Peclet number (cal) obtained from simulation (space charge model) with the experimental value.

All the data points lie on the 45° line.

Using the SCM, we determined the effective pore radius (1.0 nm for UM, 3.5 nm for 3-AEM, 6.0 for 6-AEM, and 6.5 nm for 9-AEM) and wall potential (2.1 for UM, 2.4 for 3-AEM, 4.37 for 6-AEM, and 4.15 for 9-AEM) (given in Table 1). These were determined at the point where the root mean square (rms) error, in the calculation of Peclet number (permeate flux) with the change in the value of pore radius, is a minimum.[55,56] The pore radius thus determined lies near the center of the pore size range determined by using the MWCO experiment. The pore radius determined here is the average of the actual pore radii present in the membrane. It has been averaged in such a way that the calculated values of the solute and permeate flux match with the experimentally determined values. The average pore radius thus determined is specific to the case of Cr(VI) because its permeate flux is used as the (basis) weight for determination of the average value. It can be seen from Table 1 that the pore radii are found to be less than the pore radii calculated by the MWCO experiment, which indicates a partial blocking of the pores by the solute. These results confirm that the pore size of the membrane increases with the duration of modification reaction. A decrease in the pore radius is explained by the increase in the electrical double layer thickness to cover a greater area of the pore with an increase in the charge density of the membrane by modification. Table 1 clearly shows that the wall potential of the membrane increases with increasing anion-exchange capacity. We have compared the experimental permeate flux (in nondimensional form as Peclet number) with the flux obtained from the simulation (shown in Figure 10). All the data points (both the experimental and calculated) lie on the 45 ° line, which confirms that the simulated flux matches closely with the experimental permeate flux for all the mem-

branes. Using this analysis, the membrane surface concentration (c_l) and the intrinsic rejections are calculated.

On comparing the intrinsic rejection values calculated from space-charge model with the Spiegler–Kedem relation, we find that the rejection values of the former are about 10–40% lower than those of the latter, a phenomenon explained by the concentration polarization that is taken into account by a scheme given by Ghose et al.[69] in the Spiegler–Kedem model. In the SCM, the membrane surface concentration is determined by evaluation of the applied pressure difference and matching it with the experimental value.

Conclusions

A crosslinked PMMA–EGDM clay composite anion exchange membrane has been prepared by a two-stage modification technique. The membrane prepared has been characterized in terms of pure water flux, water content, ion-exchange capacity, contact angle measurements, and membrane morphologies. The pore size, water content, ion-exchange capacity, and hydrophilicity of the modified membranes increase with the duration of modification reaction. The above-prepared membranes have been used for Cr(VI) salt solution separation and the result shows that the modified membrane gives much higher permeate flux with a rejection of 90%. We have analyzed the separation of Cr(VI) from its aqueous solution using a two-dimensional (in cylindrical coordinates) space-charge model and the effective pore size and the wall potential of these membranes are evaluated. The intrinsic rejection of the membranes determined from the space-charge model has been compared with that of the Spiegler–Kedem model.

Literature Cited

1. Mulder M. *Basic Principles of Membrane Technology*. Dordrecht, The Netherlands: Kluwer Academic; 1991.
2. Kita H, Tanaka K, Okamoto K, Yamamoto M. The esterification of oleic acid with ethanol accompanied by membrane separation. *Chem Lett*. 1987;2053-2056.
3. Rezac ME, Koros WJ. Preparation of polymer–ceramic composite membranes with thin defect-free separating layers. *J Appl Polym Sci*. 1992;46:1927-1938.
4. Yanagisita H, Kitamoto D, Haraya K, Nakane T, Tsuchiya T, Koura N. Preparation and pervaporation performance of polyimide composite membrane by vapor deposition and polymerization (VDP). *J Membr Sci*. 1997;136:121-126.
5. Hayakawa Y, Terasawa N, Hayashi E, Abe T. Plasma polymerization of cyclic perfluoroamines and composite membranes for gas separation. *J Appl Polym Sci*. 1996;62:951-954.
6. Yamaguchi T, Nakao S, Kimura S. Plasma-graft filling polymerization: Preparation of a new type of pervaporation membrane for organic liquid mixtures. *Macromolecules*. 1991;24:5522-5527.
7. Ulbricht M, Schwarz HH. Novel high performance photo-graft composite membranes for separation of organic liquids by pervaporation. *J Membr Sci*. 1997;136:25-33.
8. Zhigong R, Guixiang L, Sugo T, Okamoto J. Gas-phase and liquid-phase pre-irradiation grafting of AAc onto LDPE and HDPE films for pervaporation membranes. *Int J Radiat Appln Instrument Part C. Radiat Phys Chem*. 1992;39:421-428.
9. Peterson J, Peinemann KV. Novel polyamide composite membranes for gas separation prepared by interfacial polycondensation. *J Appl Polym Sci*. 1997;63:1557-1563.
10. Kuberkar VT, Davis RH. Microfiltration of protein cell mixtures with cross or backflushing. *J Membr Sci*. 2001;183:1-14.
11. Koops GH, Yamada S, Nakao SI. Separation of linear hydrocarbons and carboxylic from ethanol and hexane solutions by reverse osmosis. *J Membr Sci*. 2001;189:241-254.
12. Kiso Y, Kon T, Kitao T, Nishimura K. Rejection properties of alkyl phthalates with nanofiltration membranes. *J Membr Sci*. 2001;182: 205-214.
13. Joshi M, Mukherjee AK, Thakur BD. Development of a new styrene copolymer membrane for recycling of polyester fiber dyeing effluent. *J Membr Sci*. 2001;189:23-40.
14. Kim KS, Lee KH, Cho K, Park CE. Surface modification of polysulfone ultrafiltration by oxygen plasma treatment. *J Membr Sci*. 2002; 199:135-145.
15. Ruaan RC, Chou HL, Tsai HA, Wang DM, Lai JY. Factors affecting the nodule size of asymmetric PMMA membranes. *J Membr Sci*. 2001;190:135-145.
16. Cheng JH, Wang DM, Lin FC, Lai JY. Formation and gas flux of asymmetric PMMA membranes. *J Membr Sci*. 1996;109:93-107.
17. Sanders ES, Jordan SM, Subramanian R. Penetrant plasticized permeation in polymethylmethacrylate. *J Membr Sci*. 1992;74:29-36.
18. Bikson B, Nelson JK, Muruganandam N. Composite cellulose acetate/polymethyl methacrylate for blend gas separation membrane. *J Membr Sci*. 1999;94:313-328.
19. Raymond PC, Paul DB. Sorption and transport of CO_2 and CH_4 in miscible bisphenol chloral polycarbonate/polymethyl methacrylate blends. *J Polym Sci Part B: Polym Phys*. 1990;28:2103-2117.
20. Yang T, Rogers EC. Selectivity permeation of gas mixtures in surface modified PMMA/PVDF polyblend membrane. *AIChE Symp Ser*. 1989; 85:11-17.
21. Miyata T, Obata S, Uragami T. Morphological effects of microphase separation on the permselectivity for aqueous ethanol solutions of block and graft co-polymer membranes containing poly(dimethylsiloxane). *Macromolecules* 1999;32:3712-3720.
22. Inui K, Okumura H, Miyata T, Uragami T. Permeation and separation of benzene/cyclohexane mixtures through cross-linked poly(alkyl methacrylate) membranes. *J Membr Sci*. 1997;132:193-202.
23. Baird RW. Enhancement of resistance of polyethylene to seawater-promoted degradation by surface modification. *Radiat Phys Chem*. 1982;19:113.
24. Bozzi A, Chapiro A. The nature of the initiating centres for grafting in air-irradiated perfluoro polymers. *Eur Polym J*. 1987;23:255-257.
25. Hirotsu T. Water–ethanol separation by pervaporation through plasma graft polymerized membranes. *J Appl Polym Sci*. 1987;34:1159-1172.
26. Gancarz I, Pozniak G, Bryjak M. Modification of polysulfone membranes: 1. CO_2 plasma treatment. *Eur Polym J*. 1999;35:1419-1428.
27. Gancarz I, Pozniak G, Bryjak M, Frankiewicz A. Modification of polysulfone membranes. 2. Plasma grafting and plasma polymerization of acrylic acid. *Acta Polym*. 1999;50:317-327.
28. Gancarz I, Pozniak G, Bryjak M. Modification of polysulfone membranes: 3. Effect of nitrogen plasma. *Eur Polym J*. 2000;36:1563-1569.
29. Bryjak M, Gancarz I, Pozniak G, Tylus W. Modification of polysulfone membranes: 4. Ammonia plasma treatment. *Eur Polym J*. 2002; 38:717-726.
30. Kesting RE. *Synthetic Polymer Membrane: A Structural Perspective*. 2nd Edition. New York, NY: Wiley–Interscience; 1985.
31. Lin MC, Takai N. Fundamental study of non cross-linking anion exchange membranes. *J Membr Sci*. 1994;88:77.
32. Mika AM, Childs RF. A new class of polyelectrolyte-filled microfiltration membranes with environmentally controlled porosity. *J Membr Sci*. 1995;108:37.
33. Sata T, Yamane Y. Preparation and properties of anion exchange membranes having pyridinium or pyridnium derivatives as anion exchange groups. *J Polym Sci Part A: Polym Chem*. 1998;36:49.
34. Hwang GJ, Ohya H. Preparation of anion-exchange membrane based on block copolymers. Part 1. Amination of the chloromethylated polymers. *J Membr Sci*. 1998;140:195-203.
35. Hwang GJ, Ohya H. Preparation of anion exchange membrane based on block copolymers. Part II. The effect of the formation of macroreticular structure on the membrane properties. *J Membr Sci*. 1998;149: 163-169.
36. Tongwen X, Weihua Y. Fundamental studies of a new series of anion exchange membranes; membrane preparation and characterization. *J Membr Sci*. 2001;190:159-166.
37. Gzara L, Dhahbi M. Removal of chromate anions by micellar enhanced ultrafiltration using cationic surfactant. *Desalination*. 2001; 137:241-250.
38. Cassano A, Drioli E, Molinari R, Bertolutti C. Quality improvement of recycled chromium in tanning operation by membrane process. *Desalination*. 1996;108:193.

39. Cassano A, Molinari R, Droli E. Saving of water and chemicals in tanning industry by membrane separation processes. *Water Sci Technol*. 1990;40:183.
40. Pizzichini-Fabiani C, Ruscio F, Spasoni M, Pizzichini M. Chromium (III) salts recovery process from tannery wastewater. *Desalination*. 1996;108:183.
41. Neelakandan C, Pugazhenthi G, Kumar A. Preparation of NO_x modified PMMA–EGDM composite membrane for the recovery of chromium (VI). *Eur Polym J*. 2003;39:2383-2391.
42. Potdar A, Shukla A, Kumar A. Effect of gas phase modification of analcime zeolite membrane on the separation of CPC by ultrafiltration. *J Membr Sci*. 2002;210:209-225.
43. Chowdhury SR, Kumar P, Bhattacharya PK, Kumar A. Separation characteristics of modified polysulfone ultrafiltration membrane using NO_x. *Sep Purif Technol*. 2001;24:271-282.
44. Sinha S, Kumar A. Preparation of high capacity chloromethylated strong base anion exchange resin using NO_x. *Sep Sci Technol*. 2002; 37:895-919.
45. Jayaswal N, Sinha S, Kumar A. Effect of chemical modification upon exchange capacity of aminated macroporous PS–DVB copolymer anion exchange resin. *J Appl Polym Sci*. 2001;79:1735-1748.
46. Sinha S, Kumar A. Preparation of molecularly different macroporous strong base anion exchange resin of higher capacity. Proc of 6th World Congress of Chemical Engineering, Melbourne, Australia; 2001.
47. Sinha S, Jayaswal N, Kumar A. Preparation of high capacity weak base polymethyl methacrylate ethylene glycol dimethacrylate (PMMA–EGDM) copolymer anion exchange resin by modification using NO_x. *J Appl Polym Sci*. 2003;89:1991-1999.
48. Pugazhenthi G, Kumar A. Enzyme membrane reactor for hydrolysis of olive oil using lipase immobilized on modified PMMA composite membrane. *J Membr Sci*. 2004;228:187-197.
49. Breslau BR, Testa AJ, Milnes BA, Medjanis G. *Ultrafiltration Membranes and Applications*. New York, NY: Plenum Press; 1980:109-128.
50. Teorell T. An attempt to formulate a quantitative theory of membrane permeability. *Proc Soc Exp Biol Med*. 1935;33:282.
51. Meyer KH, Sievers JF. La permeabilite des membranes. I. Theory de la permeabilite ionique. *Helv Chim Acta*. 1936;19:649.
52. Hoffer E, Kedem O. Hyperfiltration in charged membranes: The fixed charge model. *Desalination*. 1967;2:25.
53. Gross RJ, Osterle JF. Membrane transport characteristics in ultrafine capillaries. *J Chem Phys*. 1968;49:228-234.
54. Fair JC, Osterle JF. Reverse electrodialysis in charged capillary membranes. *J Chem Phys*. 1963;54:328.
55. Shukla A, Kumar A. Analysis of separation of chromic acid by zeolite–clay composite membrane using space-charge model. *J Membr Sci*. 2004;237:119-130.
56. Shukla A, Kumar A. Modeling of separation of aqueous solutions of $FeCl_3$ and $AlCl_3$ by zeolite–clay composite membranes using a space-charge model. *J Colloid Interface Sci*. 2004;274:204-215.
57. Sonin A. Osmosis and ion transport in charged porous membranes: A macroscopic mechanistic approach. In: Selegny E, ed. *Charged Gels and Membranes*. Vol. 1. Dordrecht/Boston: D. Reidel, 1976:255-265.
58. Cwirko EH, Carbonell RG. Transport of electrolytes in charged pores: Analysis using the method of spatial averaging. *J Colloid Interface Sci*. 1989;129:513-531.
59. Wang X-L, Tsuru T, Nakao SI, Kimura S. Electrolyte transport through nanofiltration membranes by the space-charge model and the comparison with Teorell–Meyer–Sievers model. *J Membr Sci*. 1995; 103:117-133.
60. Neogi P, Ruckenstein E. Viscoelectric effects in reverse osmosis. *J Colloid Interface Sci*. 1981;79:159.
61. Probstein RF, Sonin AA, Yung D. Brackish water salt rejection in hyper-filtration membranes. *Desalination*. 1973;13:303.
62. Hijnen HJM, Van Daalen J, Smit JAM. The application of the space-charge model to the permeability properties of charged microporous membranes. *J Colloid Interface Sci*. 1985;107:525.
63. American Society for Testing and Materials (ASTM). ASTM 3087. Operating performances of anion exchange materials for strong acid removal, IS 7330-1998. Methods of samples and test for ion-exchange resin. Philadelphia, PA: ASTM; 1998.
64. Vanoss CJ. *Interfacial Forces in Aqueous Media*. New York, NY: Marcel Dekker; 1994.
65. Nunes SP, Peinemann KV. Ultrafiltration membranes from PVDF/PMMA blends. *J Membr Sci*. 1992;73:25-35.
66. Sasidhar V, Ruckenstein E. Electrolyte osmosis through capillaries. *J Colloid Interface Sci*. 1981;82:439-457.
67. Bhattacharryya D, Jumawan AB. Separation of toxic heavy metals by sulfide precipitation. *Sep Sci Technol*. 1979;14:441-452.
68. Bhattacharryya D, Schaaf DP. Charged membrane ultrafiltration of heavy metal salts: Application to metal recovery and water reuse. *Can J Chem Eng*. 1976;54:185.
69. Ghose S, Bhattacharjee C, Datta S. Simulation of unstirred batch ultrafiltration process based on reversible pore-plugging model. *J Membr Sci*. 2000;169:29-38.
70. Sbai M, Fievet P, Szymczyk A, Aoubiza B, Vidonne A, Foissy A. Streaming potential, electroviscous effect, pore conductivity and membrane potential for the determination of the surface potential of a ceramic ultrafiltration membrane. *J Membr Sci*. 2003;215:1-9.
71. Chen Z, Deng M, Chen Y, He G, Wu M, Wang J. Preparation and performance of cellulose acetate/polyethyleneimine blend microfiltration membranes and their applications. *J Membr Sci*. 2004;235:73-86.

Manuscript received Jun. 17, 2004, and revision received Nov. 4, 2004.